# Title
Development of Silicon Drift Detectors for Strangeness Measurements



Authors
Odyniec, G.J.
Krieger, B.
Krofcheck, D.
et al.

Publication Date
1995-02-01

LBL-36908
UC-414

**Lawrence Berkeley Laboratory**
UNIVERSITY OF CALIFORNIA

Invited paper presented at the Strangeness '95 Workshop, Tucson, AZ, January 4–6, 1995, and to be published in the Proceedings

# Development of Silicon Drift Detectors for Strangeness Measurements

G. Odyniec, B. Krieger, D. Krofcheck, D. Lewak, R. O'Donnel, M. Partlan, J.T. Walton, and N.W. Wang

February 1995



NUCLEAR SCIENCE DIVISION



Prepared for the U.S. Department of Energy under Contract Number DE-AC03-76SF00098

## DISCLAIMER

LBL-36908
UC-414

Invited paper presented at the
Strangeness '95 Workshop,
Tucson, Arizona, January 4-6, 1995

# Development of Silicon Drift Detectors for Strangeness Measurements

G. Odyniec, B. Krieger, D. Krofcheck, D. Lewak, R. O'Donnel,
M. Partlan, J.T. Walton, and N.W. Wang
Lawrence Berkeley Laboratory
University of California, Berkeley, CA 94720

February 1995

This work was supported by the Director, Office of Energy Research, Division of Nuclear Physics of the Office of High Energy and Nuclear Physics of the U.S. Department of Energy under Contract DE-AC03-76SF00098

# Development of Silicon Drift Detectors for Strangeness Measurements

G.Odyniec, B.Krieger, D.Krofcheck, D.Lewak, R.O'Donnell, M.Partlan, J.T.Walton and N.W.Wang
*Lawrence Berkeley Laboratory, University of California, 1 Cyclotron Rd., Berkeley, CA 94720*

Detection of multi-strange and charm particles requires precise measurements of the secondary vertices close to the interaction point and the decay products of strange and charm particles. This presents an unprecedented challenge for relativistic heavy ion experiments, where multiplicity reaches thousands of final state particles per collision. Development of affordable technology for realizing high spatial resolution and low mass vertex detectors has become the ultimate goal of many R&D projects in major laboratories.

In this paper we present preliminary results on silicon drift detectors fabricated for the first time on p-type silicon substrates. These detectors were designed, fabricated and tested recently at LBL and show very interesting properties which make their use in future experiments very likely.

## I. INTRODUCTION.

Strange and charm particles are potential probes of the QGP. Strange quarks, the heaviest of the abundantly produced quarks, may be enhanced during QGP formation [1]. If charm particles can be detected and measured at CERN SPS, RHIC or LHC experiments, they would determine the primordial temperature in these collisions [2], important to establishing the existence of a phase transition. Furthermore, the measurement of lifetimes, branching ratios, and especially the detection and detailed study of suppressed channels will shed light on the decay mechanism through quark graphs other than the spectator ones. The fact that the quarks are not free particles, but are bound by the strong force, implies that the study of the weak decays of particles with heavy flavors provides a testing-ground for the understanding of QCD effects in the perturbative regime. All of these rely heavily on detection and accurate measurement of the decay products of strange and charm particles.

A vertex detector with very high spatial resolution positioned close to the interaction point, in conjunction with momentum and particle identification derived from the main tracking detector of the experiment (most frequently a TPC), will most likely enable isolation of secondary vertices and determination of particle decay kinematics.

A few years ago, we performed simulations for the planned STAR experiment at RHIC [3] which demonstrated that the addition of a high precision vertex detector to the experimental set-up enhanced detection efficiency enormously for multi-strange particles. Figure 1 a and b show the invariant mass distribution ('ideal' case, without accounting for the momentum resolution) for $\Xi$ ($c\tau$=4.91cm) produced in Au+Au collisions at a total center of mass energy of 200 A GeV (RHIC), according to Fritiof event simulator, and reconstructed in (a) the STAR main tracking TPC alone and (b) the TPC with a high precision vertex detector.

The additional information from the vertex detector allowed for almost complete elimination of the background, whereas the TPC alone could only provide marginal information on $\Xi$ production, even in the so-called 'ideal' case with perfect momentum measurements. Figure 2 shows the invariant mass of $\Xi$ (main TPC + vertex detector) with a TPC momentum resolution of $\Delta p/p = 1\%$ taken into account. The peak is slightly broader, but the signal is still very strong (note different vertical scales on Figures 1 and 2). The arrows indicate the correct masses of hyperons.

Similar results were obtained for $\bar{\Xi}$'s, $\Omega$'s and $\bar{\Omega}$'s. As an example, the invariant mass plot for $\Omega$ ($c\tau$=2.46 cm) is shown in Figure 3.

In recent years, silicon strip detectors have become indispensable in high energy physics experiments. They have not, however, been applicable to high multiplicity environments due to the large number of so-called ghost hits (ambiguities of combined one-dimensional information collected from planes of the strip detectors). An ideal solution for the high multiplicity collisions existing in relativistic nucleus-nucleus interactions appears to be the large area silicon drift detectors (SiDD) proposed in 1983 by P.Rehak, E.Gatti and J.T.Walton [4] and built at LBL in the same year for the first time. SiDDs provide two-dimensional position measurements of traversing particles with high spatial and energy resolution, without ambiguities even in the presence of high particle multiplicity. Recently reported numbers are an energy resolution of 143 eV FWHM at 5.89 keV for a cooled SiDD [5] and a position resolution of a few micrometers for a room temperature SiDD [6]. Furthermore, SiDDs require an order of magnitude fewer readout channels than pixel detectors of corresponding granularity, and they introduce little material in the particle path (the typical thickness of silicon wafers used, 300 $\mu$m, corresponds to a 0.3% radiation length).

Until last year, all SiDDs had been fabricated on n-type silicon substrates. To a large extent, this was perhaps due to the fact that n-type silicon technology was well developed since it had typically been used in fabrication of other types of radiation detectors (surface barrier, silicon strip detectors, etc.). However, typical detector grade, float-zone grown, n-type silicon is not suitable for the SiDD production because of the excessively large radial variation in its

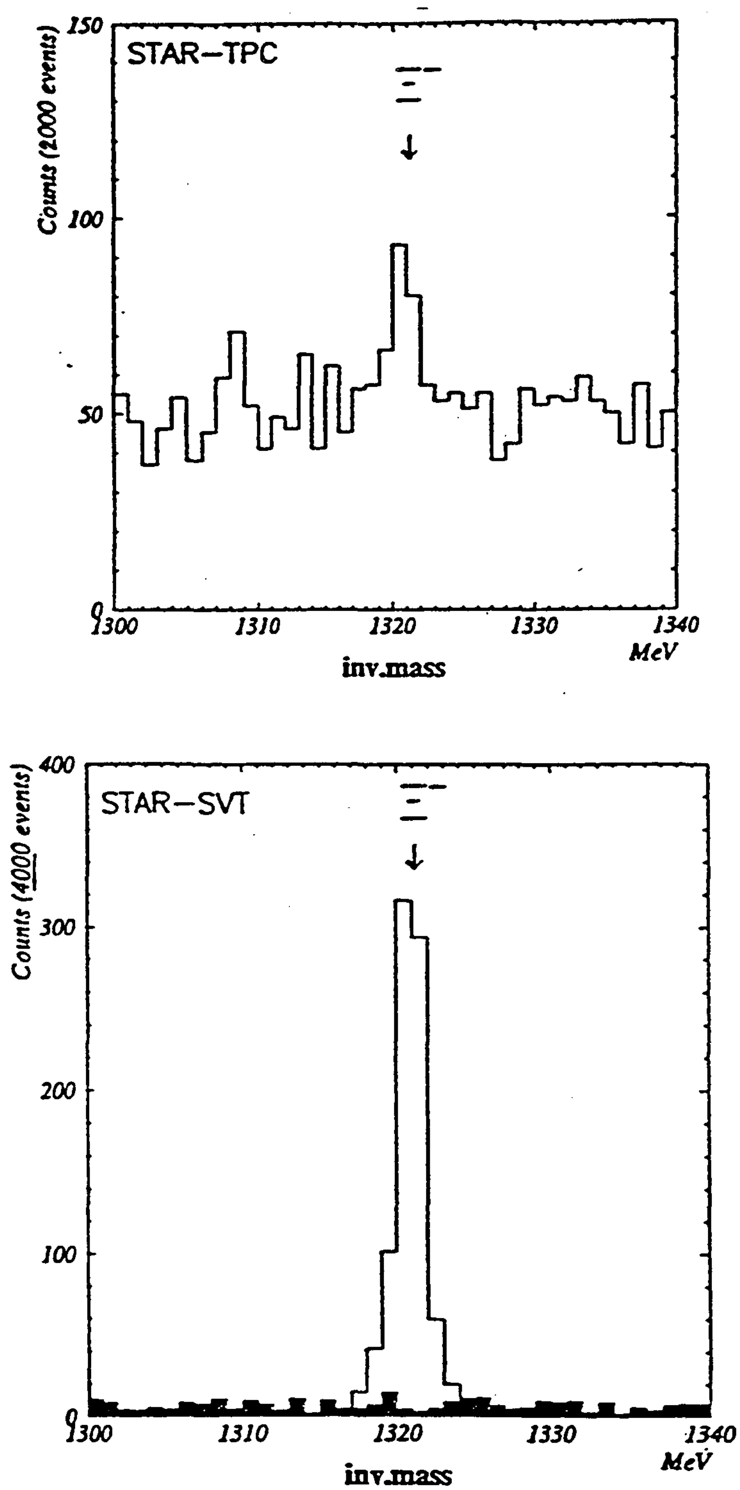


FIG. 1. Simulation of the invariant mass distributions ('ideal' case) for $\Xi$'s reconstructed in STAR TPC alone (a) and TPC with the vertex detector (b). Shaded areas represent the contribution from random background.

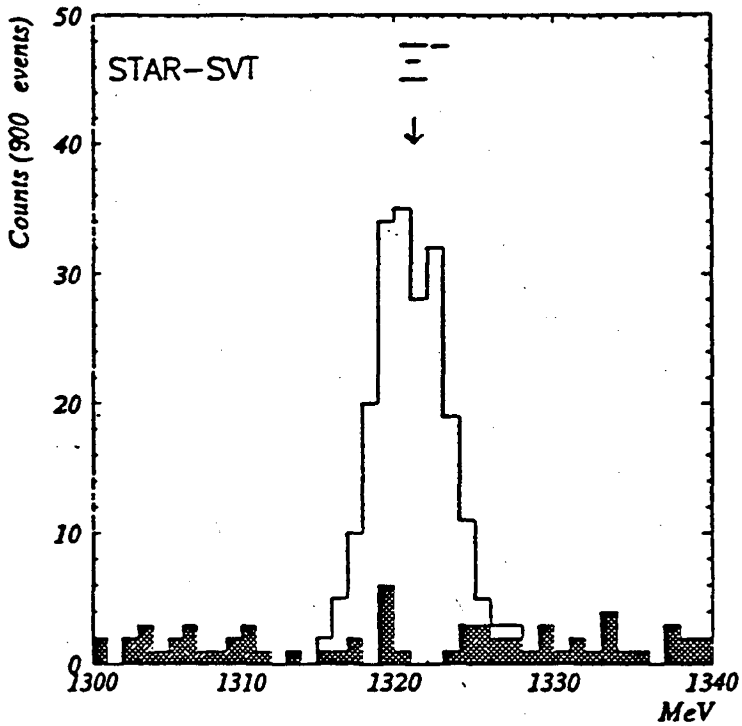


FIG. 2. Simulation of the invariant mass distributions of Ξ's (TPC + vertex detector) with TPC resolution taken into account. Shaded areas represent the contribution from random background.

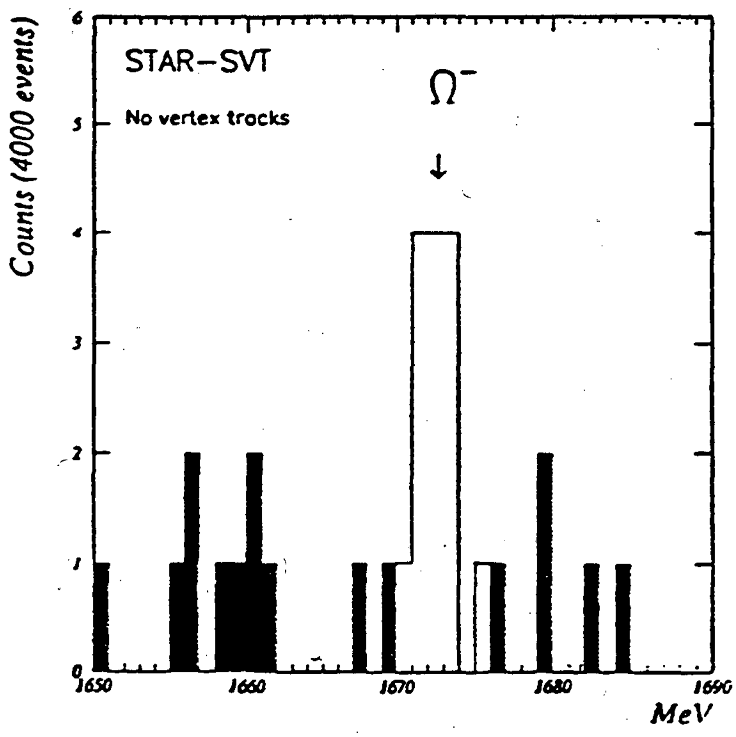


FIG. 3. Simulation of the invariant mass distributions of Ω's reconstructed in STAR TPC and vertex detector. Shaded areas represent the contribution from random background.

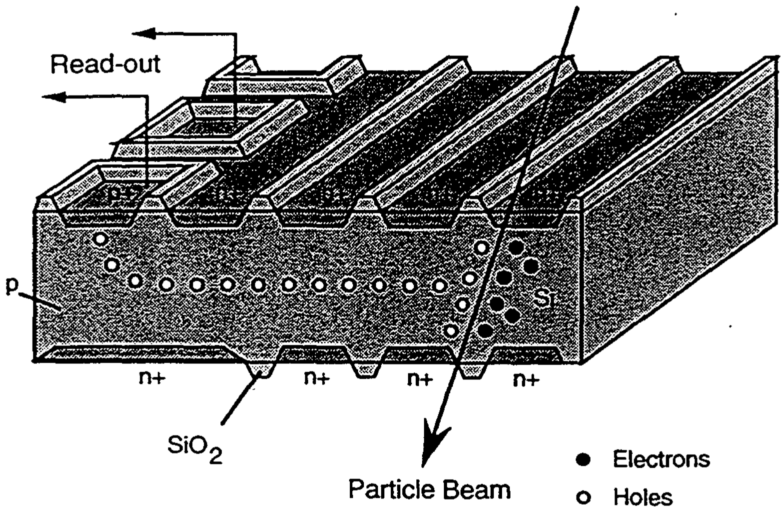


FIG. 4. Cross section of position sensitive p-SiDD. The holes created by the particle traversing the detector drift to the anodes, where they are collected.

resistivity. In order to obtain high purity, n-type silicon with the dopant uniformity required for SiDD, one has to use the neutron transmutation doping technique (NTD), in which silicon atoms are converted to phosphorus atoms very uniformly throughout the ingot by neutron bombardment. The phosphorus created in the silicon by the NTD process must be subsequently made electrically active by thermal annealing. Therefore, the resistivity of NTD silicon depends on its annealing history and can change uncontrollably during subsequent high temperature processing. This may lead to significant deviations in detector performance, and therefore the overall yield of n-type SiDDs with the desired specifications may be low. Another practical limitation comes from the fact that high resistivity NTD material is very expensive and difficult to obtain as it is manufactured only by special order.

Two years ago, our group at LBL began to examine fabrication of p-type silicon drift detectors.

Implementing SiDDs on p-type substrates offers several important advantages:

- no dependence of resistivity on thermal cycling - high purity p-type silicon does not exhibit unpredictable changes with high temperature annealing,
- readily available material - high purity p-type silicon is available 'off the shelf' at low cost, whereas n-type NTD wafers are available only by special order from one vendor, Wacker Chemitronics,
- better match to existing electronics - the slower drift velocity of holes in a p-type SiDD would, in many instances, allow existing 10-20 MHz read-out electronics to be used, whereas the higher velocity of electrons in n-type requires custom made fast electronics with 40-100 MHZ clocking,
- easier integration of front-end electronics - the p-type silicon substrate will facilitate the monolithic integration of n-channel FET's with the p-SiDD. N-channel FET's are easier to fabricate than their p-channel counterparts.

## II. DETECTOR OPERATION AND STRUCTURE.

A diagram of the cross-section of the p-SiDD is shown in Figure 4.

The device consists of parallel p-n+ junctions (the cathodes) formed on both sides of a substrate of lightly doped (e.g. $2\times10^{12}/cm^3$), ultra-high purity, p-type silicon. During device operation, the cathodes are reverse biased to deplete the entire bulk of the detector and to create a uniform electric field in the direction parallel to the surface of the silicon. When electron-hole pairs are created by a particle passing through the detector, the electrons are swept out by the reverse biased cathodes, and the holes are focused down the midplane of the detector and drift toward the collecting electrodes (the anodes). Figure 5 shows a potential map of the detector.

The transit time of the holes allows the distance of the incident particle from the anode to be calculated. The second position coordinate is obtained from the distribution of charge over the segmented anodes. The charge pulses

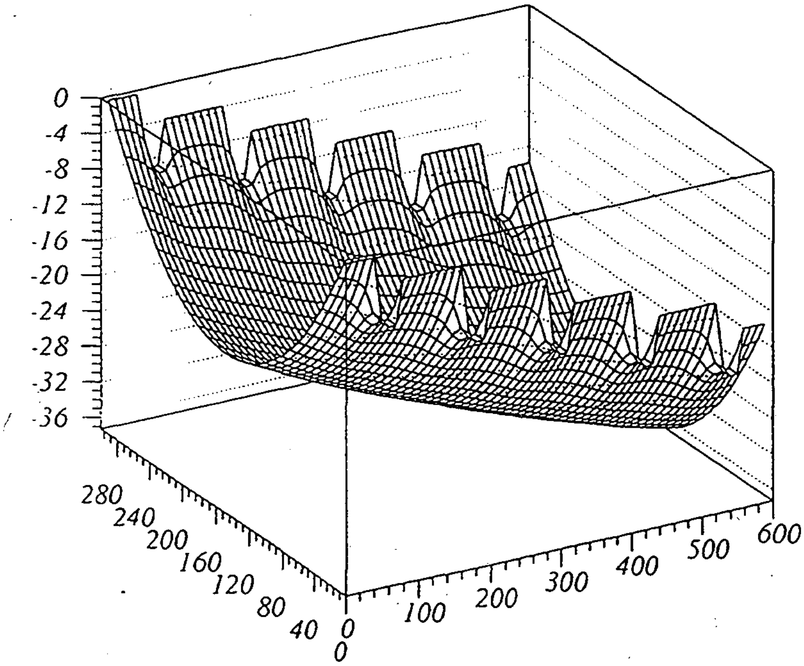


FIG. 5. The potential distribution within the p-SiDD. The bias applied to successive cathodes is stepped down to produce a potential gradient within the p-SiDD.

arriving at the anodes are amplified and sent to the read out system, then analyzed to calculate the position of the incident particle.

The geometry of our p-SiDD design is based on an n-type SiDD developed by P. Rehak at Brookhaven National Laboratory. A schematic of the detector geometry is shown in Figure 6. The active region of the detector is 3.98 cm long and consists of 332 parallel, 90 $\mu$m wide cathode strips separated by 30 $\mu$m wide $SiO_2$ regions. A high voltage guard structure of floating n+ strips surrounds three sides of the active region. The guard strips were designed to allow the potential to decrease gradually away from the biased cathodes. Since more guarding is needed around the high voltage cathodes than at the low voltage cathodes, the length of the cathodes decreases from 4.99 cm to 3.51 cm to accommodate a larger number of guard strips at the 'hot' end of the detector. At the low voltage end of the detector, there is a row of 178 rectangular p+ anodes for reading out the signals. The anodes have a pitch of 250 $\mu$m. The area of each individual anode is very small to keep the output capacitance low. Figures 7 and 8 show, respectively, the schematic of the segmented anode area of the LBL p-SiDD prototype and the electric field map in this region.

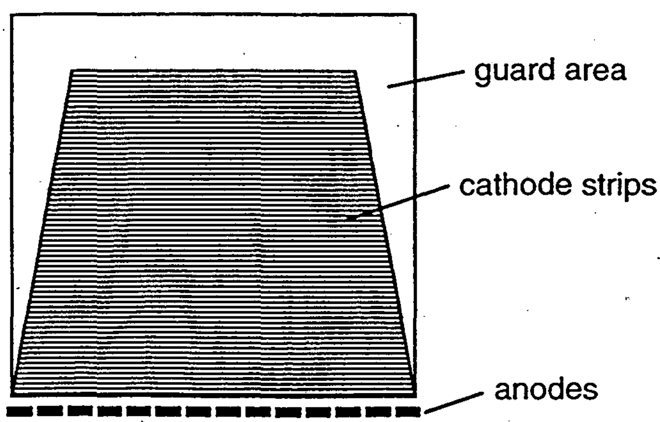


FIG. 6. Top view of the p-SiDD geometry. The cathodes and the guard region are n+ diffused strips and the anodes are p+ implanted regions.

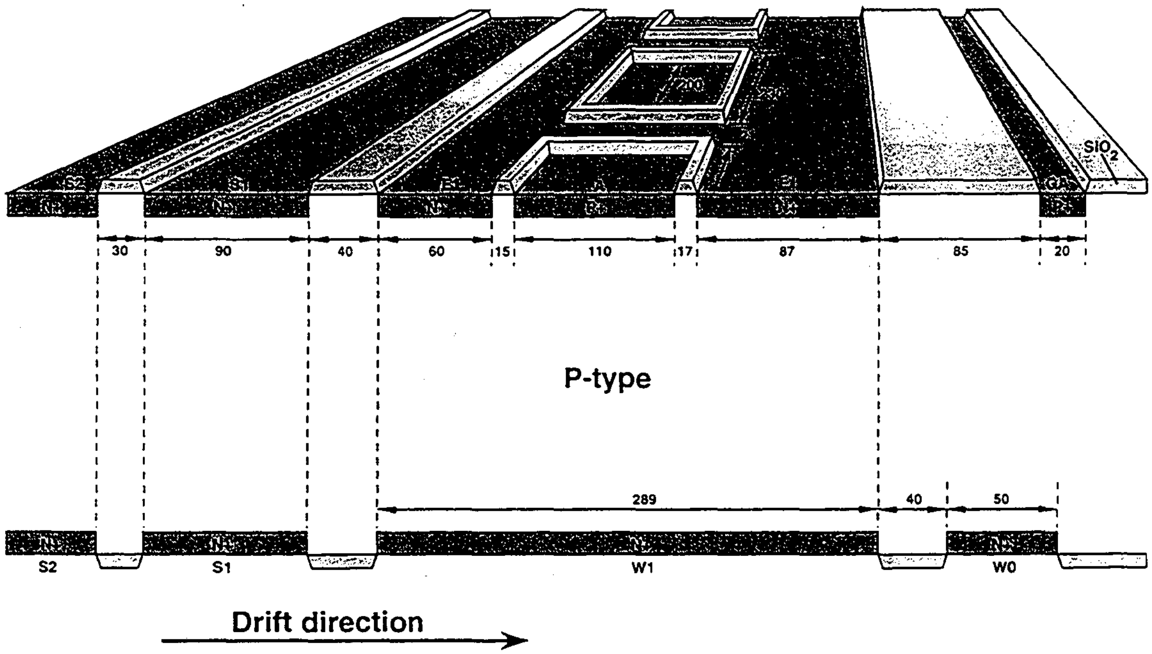


FIG. 7. Magnified cross-section through the anode region.(Distance is measured in microns.)

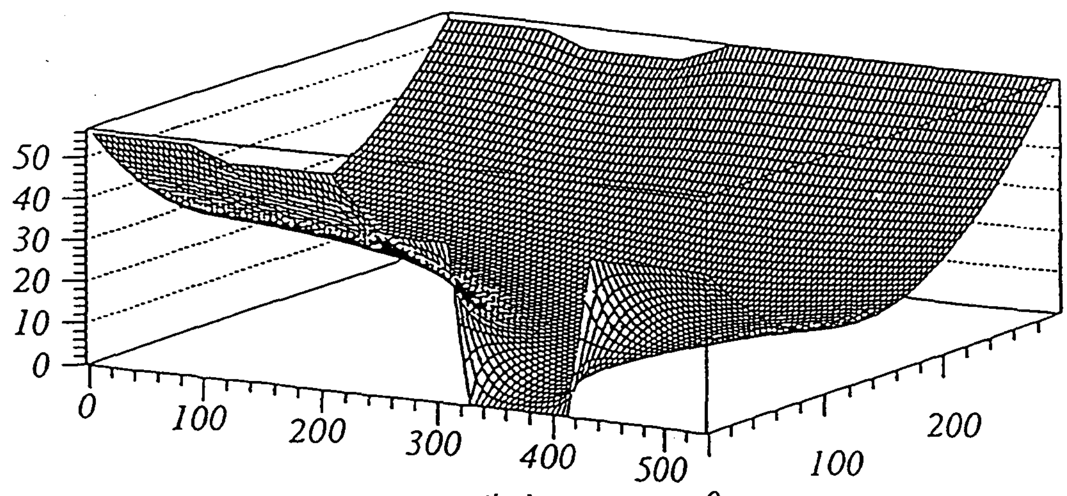


FIG. 8. The potential distribution near the collecting anode. The anode is grounded.

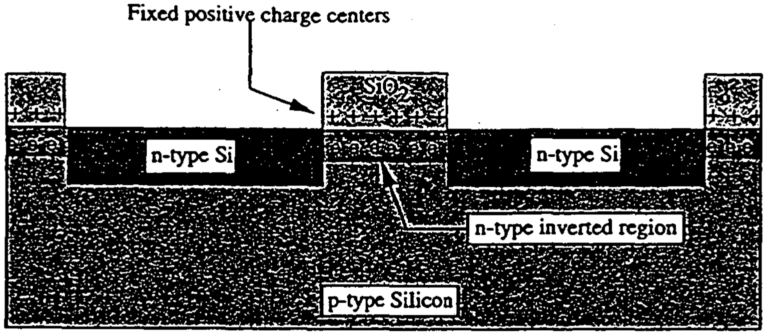


FIG. 9. Illustration of the surface inversion at the $Si/SiO_2$ interface

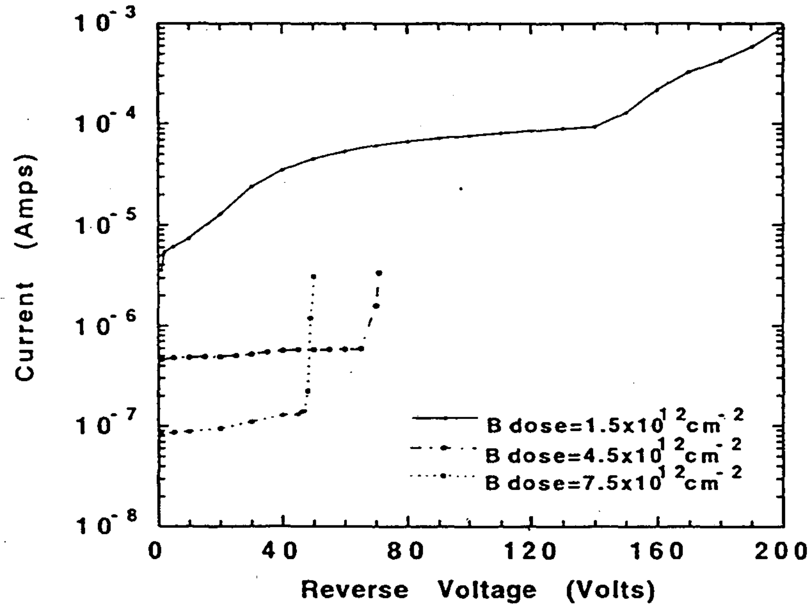


FIG. 10. Current-voltage characteristics of the p-n+ junction used to focused charge into the anode for different pre-oxidation boron implant doses.

## III. DETECTOR FABRICATION.

We fabricated the p-type SiDDs on a 3 inch diameter, 300 $\mu$m thick, float-zone, (111), p-type silicon from Wacker Chemitronics. Capacitance-voltage measurements on diodes fabricated around the periphery of the detectors showed a substrate boron density of $\sim 2 \times 10^{12}\text{cm}^{-3}$, corresponding to a bulk resistivity of $\sim$7 k$\Omega$-cm.

One of the challenges of fabricating oxide-passivated devices on high purity p-type silicon is related to the fact that positive charge at the $Si/SiO_2$ interface will attract electrons towards the wafer surface. This can result in an inversion of the carrier population at the surface from p-type to n-type, as illustrated in Figure 9.

In the p-SiDD, carrier inversion will create conducting channels between neighboring n+ cathodes. Thus, fabricating p-SiDDs with reasonably low leakage currents requires a strategy to prevent electrons from becoming the majority carrier at the $Si/SiO_2$ interface.

To prevent surface inversion, we compensated the positive oxide charge by increasing the hole concentration near the surface of the silicon with a uniform boron implant over both sides of the detector before the oxidation step [7]. However, a trade-off is involved in that, when the surface boron concentration is increased, the electric field rises at the junction and lowers the avalanche breakdown voltage. To determine an optimal boron concentration which is sufficient to compensate for the positive interface charge but which allows high breakdown voltages, we fabricated a series of detectors with different boron implant doses. A detailed discussion of the detector fabrication and implant optimization can be found in Ref. [8]. Here, we will briefly summarize the final results. The dependence of junction breakdown voltage on boron implant dose is shown in Figure 10.

The $1.5\times10^{12}$ cm$^{-2}$ implant dose was not sufficient to prevent surface inversion and resulted in very high leakage currents. The $7.5\times10^{12}$ cm$^{-2}$ implant resulted in much lower leakage currents but the breakdown voltage of 50 V

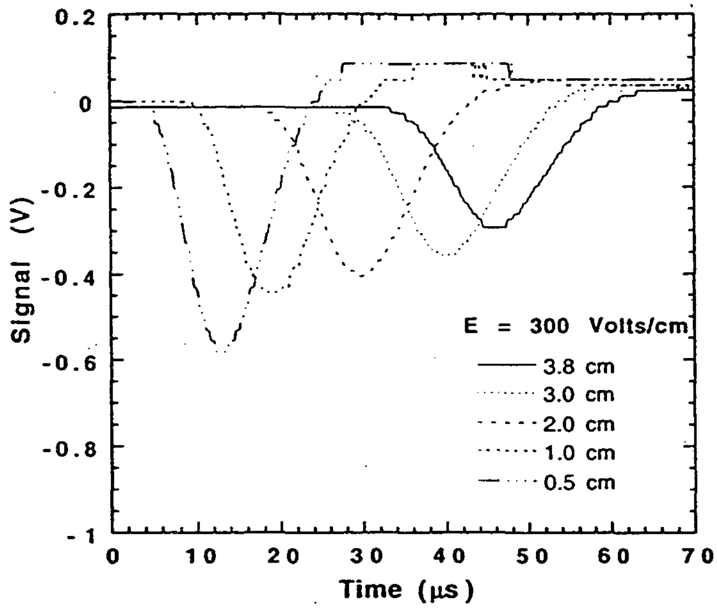


FIG. 11. Signals generated with laser focused at 0.5, 1.0, 2.0, 3.0, and 3.8 cm from the anode. Note the increase in peak time and width with drift distance.

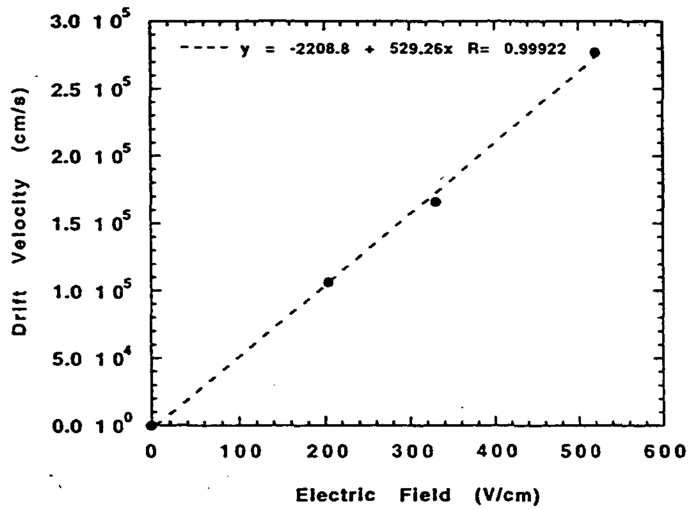


FIG. 12. Drift velocity vs. electric field.

was less than the depletion voltage of the detector. The $4.5\times10^{12}$ $cm^{-2}$ implant gave higher breakdown voltages, but measurements on these detectors were inconclusive and will be pursued further. Optimal results were obtained with detectors fabricated with a $3\times10^{12}cm^{-2}$ implant. The $3\times10^{12}cm^{-2}$ implant dose resulted in junctions with breakdown voltages of 200 V. When all the cathodes in the active area were biased, however, the highest cathode on the same detector could withstand up to 1300 V without breakdown corresponding to a drift field of 325 V/cm. This shows that the high voltage guard structure is effective in suppressing high local fields which lead to breakdown.

For position-sensitive testing, the detectors were positioned on a computer-controlled x-y stage with a 0.5$\mu$m step. Weakly absorbed, 1.06$\mu$m light from a pulsed Nd:YAG laser was focused through a microscope objective to a 5$\mu$m diameter spot on the detector surface. An external resistor voltage divider supplied voltages to the cathodes. The anodes were individually read out through discrete preamplifiers and shaping amplifiers.

Figure 11 shows signals measured with the laser focused at 0.5, 1.0, 2.0, 3.0, and 3.8 cm from the collecting anode. Note that the laser peaking time increases as the laser is moved farther from the anode. This demonstrates that charge generated farther from the anode takes longer to drift and be collected at the anode. Note also the increase in the signal width at larger drift distances. This is due to the longer collection time during which the charge packet diffuses. A plot of the drift velocity at four different electric fields is shown in Figure 12.

The hole mobility calculated from these drift measurements was 526 $cm^2$/V-sec. This agrees well with the expected mobility value of 498 $cm^2$/ V-sec at 22°C.

## IV. CONCLUSIONS.

We have fabricated, for the first time, a silicon drift detector using p-type silicon as the starting material. A uniform boron implant of $3\times10^{12}$ $cm^{-2}$ before oxidation has been demonstrated to effectively prevent surface inversion due to positive fixed oxide charge while allowing voltages of up to 1300 V to be applied to the detectors without breakdown. Drift measurements conducted for electric fields of up to 520 V/cm show that the signal transit time is linear with position for these devices. The measured hole mobility agrees with the predicted value to within 10%. These preliminary results are very promising.

The existence of SiDD technology which uses commercially available and inexpensive high resistivity p-type silicon should facilitate the building of complex vertex detector systems for the detection of short lived particles in high multiplicity environments. This will allow us experimentally to explore previously inaccessible areas of the physics of heavy ion collisions.

Future p-SiDD development will include the integration of bias and preamplifier electronics to the detector structure, a self-triggering mechanism, and an improved high voltage guard structure. Finally, of particular interest for the large detector systems is the possibility of using the fast cathode signal (available in about 10 ns after collision occurs) as a fast multiplicity trigger for the entire experiment.

---

This work was supported by the Director, Office of Energy Research, Division of Nuclear Physics of the Office of High Energy and Nuclear Physics of the U.S. Department of Energy under Contract DE-AC03-76SF00098

[1] B.Muller,p.739, "Hadronic Matter in Collisions 1988", World Scientific, 1989, editors P.Carruthers and J.Rafelski.
[2] E.V.Shuryal, Sov.J.Nucl.Phys. 28 (3) 1978, 408 and Phys.Lett.B 215 (1988) 375 and Phys.Lett.B 233 (1989) 231.
[3] G.Odyniec et al., LBL-31773, January 1992.
[4] E.Gatti, P.Rehak and J.T.Walton , NIM 226 (1984) 129.
[5] C.Gauthier et al., NIM, A349, p.258, 1994.
[6] E.Gatti, P.Rehak and M.Sampietro, NIM, A274, p.469, 1989.
[7] J.T.Walton and F.S.Goulding, IEEE Trans.Nucl.Sci., 1, p.396, 1987.
[8] N.W.Wang et al., submitted to IEEE Trans.Nucl.Sci., 1995.

LAWRENCE BERKELEY LABORATORY
UNIVERSITY OF CALIFORNIA
TECHNICAL AND ELECTRONIC
INFORMATION DEPARTMENT
BERKELEY, CALIFORNIA 94720